# Hydrogen peroxide in the marine atmospheric boundary layer during the Atlantic Stratocumulus Transition Experiment/ Marine Aerosol and Gas Exchange experiment in the eastern subtropical North Atlantic

Daniel Martin, Maria Tsivou, Bernard Bonsang, Christian Abonnel, Thomas Carsey, Margie Springer-Young, Alex Pszenny, Karsten Suhre

▶ **To cite this version:**

Daniel Martin, Maria Tsivou, Bernard Bonsang, Christian Abonnel, Thomas Carsey, et al.. Hydrogen peroxide in the marine atmospheric boundary layer during the Atlantic Stratocumulus Transition Experiment/ Marine Aerosol and Gas Exchange experiment in the eastern subtropical North Atlantic. Journal of Geophysical Research: Atmospheres, 1997, 102 (D5), pp.6003-6015. 10.1029/96JD03056 . hal-03357865

**HAL Id: hal-03357865**
**https://hal.science/hal-03357865**

Submitted on 29 Sep 2021

**HAL** is a multi-disciplinary open access archive for the deposit and dissemination of scientific research documents, whether they are published or not. The documents may come from teaching and research institutions in France or abroad, or from public or private research centers.

L'archive ouverte pluridisciplinaire **HAL**, est destinée au dépôt et à la diffusion de documents scientifiques de niveau recherche, publiés ou non, émanant des établissements d'enseignement et de recherche français ou étrangers, des laboratoires publics ou privés.

JOURNAL OF GEOPHYSICAL RESEARCH, VOL. 102, NO. D5, PAGES 6003–6015, MARCH 20, 1997

# Hydrogen peroxide in the marine atmospheric boundary layer during the Atlantic Stratocumulus Transition Experiment/ Marine Aerosol and Gas Exchange experiment in the eastern subtropical North Atlantic

Daniel Martin,[1] Maria Tsivou,[2] Bernard Bonsang,[2] Christian Abonnel,[3] Thomas Carsey,[4] Margie Springer-Young,[4] Alex Pszenny,[45] and Karsten Suhre[6]

**Abstract.** Gas phase $H_2O_2$ was measured in surface air on the NOAA ship *Malcolm Baldrige* from June 8 to 27, 1992 (Julian days 160–179), during the Atlantic Stratocumulus Transition Experiment/Marine Aerosol and Gas Exchange experiment in the eastern subtropical North Atlantic region. Average $H_2O_2$ mixing ratios observed were 0.63 ± 0.28 ppbv, ranging between detection limit and 1.5 ppbv. For the entire experiment, only weak or no correlation was found between $H_2O_2$ mixing ratio and meteorological parameters (pressure, temperature, humidity, or UV radiation flux) as well as with tracers of continental air masses (CO, black carbon, radon). The average daily $H_2O_2$ cycle for the entire period exhibits a maximum of 0.8 ± 0.3 ppbv near sunset and a minimum of 0.4 ± 0.2 ppbv 4–5 hours after sunrise. Several clear $H_2O_2$ diurnal variations have been observed, from which a first-order removal rate of about $1 \times 10^{-5}$ $s^{-1}$ for $H_2O_2$ can be inferred from nighttime measurements. This rate compares well with those deduced from measurements taken at Cape Grim (Tasmania, 41°S) and during the Soviet-American Gas and Aerosol III experiment (equatorial Pacific Ocean).

## Introduction

The determination of hydrogen peroxide ($H_2O_2$) mixing ratio in the gas phase on a global scale is of interest in atmospheric chemistry investigations for several reasons. First, $H_2O_2$ and ozone ($O_3$) are considered to be the major oxidants of sulfur dioxide ($SO_2$) in the liquid phase (rain, cloud droplets), leading to sulfuric acid. Previous investigations [*Penkett et al.*, 1979; *Calvert et al.*, 1985] have shown that $H_2O_2$ is the predominant oxidant for *p*H lower than 5, while $O_3$ is the major oxidant at *p*H greater than 5. It has been observed [*Daum et al.*, 1984; *Finlayson-Pitts and Pitts*, 1986] that the *p*H of rain or cloud droplets over western Europe and eastern North America is usually less than 5. This suggests that $H_2O_2$ plays an important role in $SO_2$ oxidation over these regions. The second crucial role of $H_2O_2$ is as a reservoir species in the odd hydrogen family (H·, ·OH, $HO_2^{\cdot}$) [e.g., *Van Valin et al.*, 1990; *Heikes*, 1992]. These radicals are key species in atmospheric chemistry because they are directly involved in the sulfur, nitrogen, and carbon oxidation chains. As a consequence, $H_2O_2$ can be considered as a diagnostic compound of gas phase photochemistry and can be used to constrain photochemical models [e.g., *Dollard et al.*, 1989]. Furthermore, because $H_2O_2$ production from $HO_2$ radicals competes with $HNO_3$ production, $H_2O_2$ can be also considered as a clean air mass tracer [*Heikes*, 1992]. Finally, adverse effects of $H_2O_2$ on plants can occur [*Gaffney et al.*, 1987] and can be severe when $H_2O_2$ is abundant in the aqueous phase [*Masuch et al.*, 1986], although the possible impact of gaseous $H_2O_2$ has not yet been clearly demonstrated [*Dollard and Davies*, 1992].

Hydrogen peroxide is one of many compounds produced by atmospheric photochemical processes. In the gas phase, $H_2O_2$ is mainly produced by hydroperoxy radical recombination:

$$HO_2^{\cdot} + HO_2^{\cdot} \rightarrow H_2O_2 + O_2 \qquad \text{(R1)}$$

Production of $H_2O_2$ is therefore linked directly to $HO_2^{\cdot}$ concentration. The rate constant of (R1) depends on temperature and water vapor mixing ratio [*Cox and Burrows*, 1979]. Water vapor reaction with $HO_2^{\cdot}$ initiates a complex chain [*Hamilton and Lii*, 1977; *Calvert and Stockwell*, 1983] which accelerates $H_2O_2$ production:

$$HO_2^{\cdot} + H_2O \rightarrow HO_2^{\cdot} \cdot H_2O \qquad \text{(R2)}$$

$$HO_2 \cdot H_2O + HO_2^{\cdot} \rightarrow H_2O_2 + H_2O + O_2 \qquad \text{(R3)}$$

$$2(HO_2^{\cdot} \cdot H_2O) \rightarrow H_2O_2 + 2\,H_2O + O_2 \qquad \text{(R4)}$$

$HO_2^{\cdot}$ is produced through ozone photodissociation according to the following reaction scheme [*Daum et al.*, 1990; *Ayers et al.*, 1992]:

$$O_3 + h\nu\ (\lambda < 310\ \text{nm}) \rightarrow O(^1D) + O_2 \qquad \text{(R5)}$$

$$O(^1D) + H_2O \rightarrow 2 \cdot OH \qquad \text{(R6)}$$

[1]METEO-FRANCE, presently at Centre National de la Recherche Scientifique, Centre des Faibles Radio-activités, Gif sur Yvette.
[2]Centre National de la Recherche Scientifique, Centre des Faibles Radio-activités, Gif sur Yvette, France.
[3]METEO-FRANCE, Centre National de la Recherche Météorologique, Centre d'Aviation Météorologique, Brétigny sur Orge.
[4]National Oceanic and Atmospheric Administration, Atlantic Oceanographic and Meteorological Laboratory, Miami, Florida.
[5]Now at IGAC Core Project Office, Massachusetts Institute of Technology, Cambridge.
[6]Laboratoire d'Aérologie (UMR CNRS/UPS 5560), Observatoire Midi Pyrénées, Toulouse, France.

Copyright 1997 by the American Geophysical Union.

Paper number 96JD03056.
0148-0227/97/96JD-03056$09.00

$$\cdot OH + CO \rightarrow H\cdot + CO_2 \quad (R7)$$

$$H\cdot + O_2 + M \rightarrow HO_2^{\cdot} \quad (R8)$$

and from photodissociation of formaldehyde [*Calvert et al.*, 1983]:

$$HCHO + h\nu\ (\lambda < 370\ nm) \rightarrow HCO\cdot + H\cdot \quad (R9)$$

followed by (R8) and

$$HCO\cdot + O_2 \rightarrow HO_2^{\cdot} + CO \quad (R10)$$

The reaction of ozone with biogenic hydrocarbons (isoprene, terpenes) also can lead to $H_2O_2$ formation in forest areas [*Becker*, 1990].

$$O_3 + \text{terpenes} \rightarrow H_2O_2 + \text{organic compounds} \quad (R11)$$

$NO_x$ plays a crucial role in the atmospheric photochemistry of $H_2O_2$ [*Ehhalt and Drummond*, 1981; *Finlayson-Pitts et al.*, 1986; *Kleinman*, 1991]. In $NO_x$ rich air (few hundred ppt(v)), the production of $H_2O_2$ by (R1) competes with

$$HO_2^{\cdot} + NO \rightarrow \cdot OH + NO_2 \quad (R13)$$

$$NO_2 + \cdot OH + M \rightarrow HNO_3 + M \quad (R14)$$

In $NO_x$ poor air, (R13) becomes negligible with respect to (R1) and (R15) [*Gunz et al.*, 1990; *Ayers et al.*, 1992]:

$$HO_2^{\cdot} + O_3 \rightarrow \cdot OH + 2\ O_2 \quad (R15)$$

Sinks in the gas phase are (R16) and (R17).

$$H_2O_2 + \cdot OH \rightarrow H_2O + HO_2^{\cdot} \quad (R16)$$

$$H_2O_2 + h\nu\ (\lambda < 365\ nm) \rightarrow 2\cdot OH \quad (R17)$$

In clean air with low aerosol burden, these reactions are the main photochemical sink of $H_2O_2$; but in the marine boundary layer (MBL), the removal of $H_2O_2$ could be augmented by and potentially exceeded by physical processes such as dry deposition, incorporation into cloud droplets and aerosols, and scavenging by precipitation [*Logan et al.*, 1981; *Walcek*, 1987; *Kleinman*, 1986].

In this paper, we present the results of $H_2O_2$ mixing ratio measurements made aboard NOAA ship *Malcolm Baldrige*, hereinafter referred to as MB, during the Atlantic Stratocumulus Transition Experiment/Marine Aerosol and Gas Exchange (ASTEX/MAGE) experiment. Our objective here is to describe the data set and discuss the temporal variability of gaseous $H_2O_2$ observed in the marine boundary layer within the context of the production and removal processes described above.

## Experiment

Hydrogen peroxide mixing ratio measurements were made continuously aboard NOAA ship *Malcolm Baldrige* (MB) from June 8 to 27, 1992 (Julian days 160–179). Hereinafter, Julian days will be referred to as JD. The measurements were made with an automatic analyzer (AL1002 model) manufactured by AEROLASER (Germany) set in a special container on the flying bridge approximately 15 m above the ship's waterline. The sampling line consisted of a 1/4″ Teflon FEP line of 5 m length extending above the deck. The device used the fluorimetric method described in detail by *Lazrus et al.* [1986] to determine $H_2O_2$ mixing ratios. The analytical technique is based on the decomposition of peroxides by *p*-hydroxyphenylacetic acid under the catalysis by the peroxydase and measurement of the resulting fluorescence. In order to distinguish $H_2O_2$ from organic peroxides, which both contribute to the fluorescence signal, $H_2O_2$ is selectively destroyed in a second channel by the catalase. The contribution of $H_2O_2$ is determined by the difference between the channel signals. A detailed description of the instrument can be found in the work of *Weller et al.* [1993]. The detection limit of the instrument is approximately 50 pptv.

Internal calibration of the instrument is based on a permeation tube (1/16″ Teflon line) in a stabilized 30% v/v $H_2O_2$ aqueous solution maintained at constant temperature in a permeation cell. The $H_2O_2$ solution was initially calibrated against standard potassium permanganate solution ($2 \times 10^{-3}$ N) at the beginning of the cruise. The permeation rate was measured directly on JD 160 and between 174.77 and 174.83 by flowing zero air into the permeation cell, then bubbling through ultrapure deionized $H_2O$. The permeation rate was determined by comparing the response of the solution produced to that of freshly prepared $1 \times 10^{-6}$ M $H_2O_2$ solution. These permeation rates were, 4.9 and 5.38 ng $H_2O_2$ $min^{-1}$, respectively. These values, a factor of 2 lower than the permeation rates specified by the manufacturer, were used for computing $H_2O_2$ mixing ratios.

Gas phase $H_2O_2$ data were recorded on a strip chart and manually read off as 30-min averages. The accuracy of our measurements is estimated to be ±100 pptv. Because of a partial destruction of organic peroxides by catalase, *Heikes* [1989] suggested that corrections of 10% to 15% should be applied to the raw data [*Weller et al.*, 1993]. Because it is difficult to evaluate these corrections precisely, we have not applied them to our data.

Aerosol black carbon was measured with an aethalometer [*Hansen et al.*, 1990] set to take readings at 5-min intervals. Air was fed to the instrument at a flow rate of 20 ± 1 standard liter per minute (slpm) through approximately 10 m of polypropylene tubing suspended on a cable running aft from the bow tower. The inlet of the tubing was approximately 16 m above the waterline, 10 m aft of the forward bulwark, and fitted with a rain shield made from a 125-ml polyethylene bottle from which the bottom had been removed. Raw data were recorded on a computer. Off line, the four light attenuation data series were smoothed individually using a nine-point moving average, and these smoothed values were then used in the algorithm supplied by the instrument manufacturer (Magee Scientific, Inc.) to calculate black carbon concentrations. A value of 19 $m^2$ $g^{-1}$ was used for the specific attenuation of black carbon on the quartz fibber filters used (Pallflex Tissuequartz 2500 QAT-UP). The active collecting area of the filters was 0.9 $cm^2$. The filter was replaced with a new one at least once per day.

Concentrations of $^{222}Rn$ were estimated indirectly via assay of the nuclide's short-lived, β-particle emitting daughters ($^{214}Pb$ and $^{214}Bi$) in aerosols with a system based on the design of *Larson and Bressan* [1978]. Air was drawn through a 10-cm diameter glass fibber filter (Schleicher & Schuell, No. 29) for the first 20 min of an 80-min cycle at a flow rate of 0.7 $m^3$ $min^{-1}$. β-particles were then counted during four 10-min intervals beginning at 1, 11, 40, and 50 min after sampling stopped. The detector face was centred approximately 1.5 cm from the filter surface and was shielded from visible light by covering it with aluminium foil. The filter-detector assembly was housed in a box secured on a weather deck just forward of

and below the ship's navigation bridge. Variations in detection efficiency were monitored by counting sources of $^{90}Sr$-$^{90}Y$, $^{210}Pb$-$^{210}Bi$, $^{36}Cl$, and $^{99}Tc$ (Dupont NES-261, -200F, -200D, and 200-B, respectively) centered in fixed geometry in circular plastic frames that were placed individually in the filter holder for 2 to 3 min during the daily filter change interval. These data revealed a strong negative dependence of detection efficiency on temperature inside the box that housed the filter-detector assembly. Corrections were possible up to a box temperature of 30°C but resulted in uncertainties of approximately ±30% in estimated $^{222}Rn$ concentrations. Conversion of counting data to $^{222}Rn$ concentrations was based on *Bateman*'s [1910] method.

Ambient air samples for CO measurements were collected manually from the windward bow at ~10 m above sea level with a 25-ml, gas-tight, glass syringe covered by black tape. They were injected into a Carle gas chromatograph fitted with an analytical column of 5A molecular sieve. CO concentrations were determined by an attached HgO reduction detector using methods and techniques for samples and standards described by *Piotrowicz et al.* [1990].

## Results and Discussion

We explore several aspects of the data. First, we summarize the data for the whole period from JD 160 to JD 179 (June 8–27). Then, to understand the variability of the $H_2O_2$ mixing ratio, we analyze the data according to the origin of the air masses as defined by *Carsey et al.* [1994] and also by dividing the data set into three periods characterized by the presence of a clear diurnal variation of $H_2O_2$.

Finally, we derive a first-order rate constant of physical removal of $H_2O_2$ from those episodes showing a diurnal variation of $H_2O_2$.

### Summary of Data Obtained During JD 160–179 (June 8–27)

All data discussed here have been taken during JD 160 and JD 179 when the MB vessel was moving latitudinally between 27°N and 37°N and longitudinally between 22°W and 26°W in the so-called ASTEX/MAGE triangle [*Huebert et al.*, 1996].

The time series of $H_2O_2$ gas phase mixing ratios measured during the entire cruise is shown in Figure 1. Figure 2 shows the distribution of the data for the whole period ($n$ = 631). For this whole period the distribution of $H_2O_2$ mixing ratio is lognormal as shown by the statistical summary of the data given in Table 1. Ninety-five percent of the measured $H_2O_2$ mixing ratios are in the range of 0.25–1.2 ppbv with a mean value of 0.63 ± 0.28 ppbv. No measurements have been performed between JD 162.3 and JD 165.0 (June 10–13) when the ship was downwind of Santa Maria Island (Azores).

Average $H_2O_2$ mixing ratio are in good agreement with those reported by *Jacob and Klockow* [1992] and *Weller et al.* [1993] for the same latitudes over the Atlantic Ocean. They measured 0.96 ppb during fall and 0.5–0.7 ppb in winter, respectively.

Short timescale variations (i.e., less than 2 hours) can be explained by precipitation events, due to the high solubility of $H_2O_2$ in rainwater. Eleven rain events (drizzles or showers) were encountered during the June 8–27 period (marked in Figure 1 by vertical arrows and small triangles when $H_2O_2$ data were available). A rapid decrease of $H_2O_2$ can be observed after each event except when only light drizzle occurred (events on JD 166) or when $H_2O_2$ was already below detection limit (e.g., event on JD 179).

The $H_2O_2$ peak (1.5 ppbv) observed on JD 165.95 can probably be accounted for by input from the free troposphere, where $H_2O_2$ mixing ratios are typically higher than in the marine boundary layer mainly due to the absence of heterogeneous loss processes [*Heikes*, 1992]. The estimation of the strength of these processes are one scope of the present paper and will be discussed later.

The climatological three-dimensional global model described by *Kanakidou and Crutzen* [1993] and performed with ethane ($C_2H_6$) and propane ($C_3H_8$) chemistry and standard emissions predicts surface mixing ratios of about 0.65 ppbv for June at 35°N (M. Kanakidou, personal communication, 1996). Near-surface mixing ratios calculated by *Logan et al.* [1981] for 35°N latitude in summer are of the order of 0.7 ppbv. These values agree very well with our June average value of 0.63 ± 0.28 ppbv.

During the field experiment, two intensive Lagrangian experiments were performed [see *Huebert et al.*, 1996] which were carried out mainly by aircraft, the *Malcolm Baldrige* being positioned at the "end point" of each Lagrangian trajectory. Meteorological conditions during ASTEX/MAGE Lagrangian experiments have been analyzed by *Bretherton et al.* [1995]. These two periods are referred to as lag 1 (JD 164.5–166.5, June 12–14) and lag 2 (JD 170.8–172.8, June 18–20), respectively.

As the *Malcolm Baldrige* itself was not attempting to move with the wind during lag 1 and lag 2, it is not possible to analyze the behavior of $H_2O_2$ in a Lagrangian context. We have just marked these two periods in Figure 1 by diamonds (lag 1) and circles (lag 2). Finally, we note that the highest value of $H_2O_2$ (1.5 ppbv) has been observed during lag 1 JD 165.95.

### Correlation With Passive Tracers and Air Mass Origin

Is $H_2O_2$ a tracer for clean air masses? Is has been pointed out above that the $H_2O_2$ production competes with the $HNO_3$ production through (R1) and (R13). We can expect that in polluted air masses with high $NO_x$ levels, $H_2O_2$ mixing ratio would be lower than in clean air masses (low $NO_x$ regime). As a consequence, $H_2O_2$ would be a good candidate as a tracer of clean air masses [*Ehhalt and Drummond*, 1981]. We are going to explore this aspect of $H_2O_2$ using correlation with well-known passive tracers as radon 222 ($^{222}Rn$), black carbon, and carbon monoxide (CO), using in addition air mass back trajectories.

It is well known that $^{222}Rn$ is emitted primarily from land surfaces. Because its half-life is 3.8 days, it is considered one of the best tracers of continental air masses over open ocean regions. Black carbon is produced by incomplete combustion. Its background concentration over the northern hemisphere is about 15 ng $m^{-3}$ [*Cachier et al.*, 1990; *Liousse*, 1990]; significantly higher concentrations of this tracer are indicative of combustion. Another useful tracer of polluted air masses is carbon monoxide. It is produced by combustion of fossil fuels and its lifetime is about 2 months. Its mixing ratio over the North Atlantic Ocean has been observed to vary from about 75 to over 200 ppbv [*Seiler*, 1974; *Koppman et al.*, 1992; *Piotrowicz et al.*, 1990].

Observed $^{222}Rn$ concentrations vary between 10 and 30 pCi $m^{-3}$; those of black carbon are lower than 25 ng $m^3$, and those of CO vary between 80 and 140 ppbv.

If no $^{222}Rn$, black carbon, or CO data were available for a

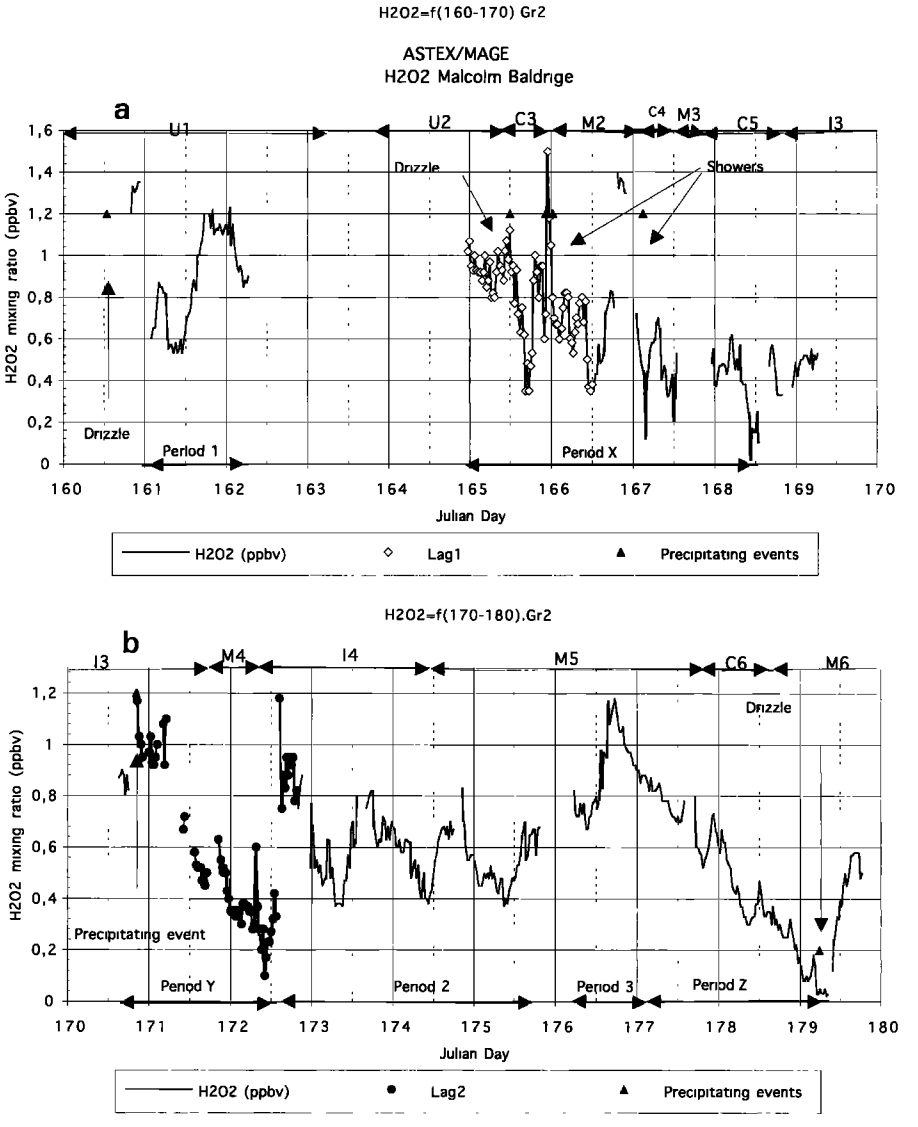


**Figure 1.** Gas phase $H_2O_2$ mixing ratio data time series for (a) Julian days 160–170 and (b) 170–180. Meterological periods are marked on the upper bound [after *Carsey et al.*, 1992]. On the lower bound, periods 1, 2, 3 show a diurnal cycle, while periods X, Y, Z show a decreasing trend.

particular $H_2O_2$ measurement, the corresponding concentration of the missing species has been estimated using linear interpolation between the two closest available $^{222}Rn$, black carbon, or CO measurements, and this only if the temporal difference between these measurements and the actual $H_2O_2$ measurement has been smaller than 45 min. Otherwise, the data point has been discarded in the correlation calculations.

Over the whole period (JD = 160–179), no significant correlation has been found neither between $H_2O_2$ and $^{222}Rn$ nor between $H_2O_2$ and black carbon (with a respective correlation coefficient of 0.11 and 0.13). For CO, a very low correlation has been observed ($r$ = 0.29) during this period. While the average concentrations of these passive tracers, calculated over the entire set of data for a given situation, are consistent with the origin of the air mass as derived from back trajectories, no significant correlation between these parameters and $H_2O_2$ except in one case when air masses came from Europe (type I of Table 2). In this case, $R_{CO}$ = 0.63 (31 data points), and $R_{bc}$ = 0.54 (40 data points).

Using back trajectory analysis and atmospheric chemistry measurements (black carbon to CO ratio), *Carsey et al.* [1994] defined four typical origins of the air sampled during the 1992 ASTEX/MAGE cruise. These different meteorological periods are reported on the upper bound of Figure 1 and are referred to uninhabited North America and United States (U), clean marine (C), mixed clean marine, and North America or Europe (M) and North Europe/North Africa (I). These selected meteorological periods are reported in Table 2.

We have calculated average $H_2O_2$ mixing ratio for each of the above meteorological periods. They all range within 0.6–0.7 ppb and are thus very close to the average value over the whole JD 160–179 period. There is no typical value of the $H_2O_2$ mixing ratio corresponding to specific type of meteorological period. Note that air masses sampled during ASTEX/MAGE typically have been over the ocean for more than 2 days. This means that even for air originating from polluted European regions, there has been enough time for processing primary atmospheric pollutants and that we cannot expect to

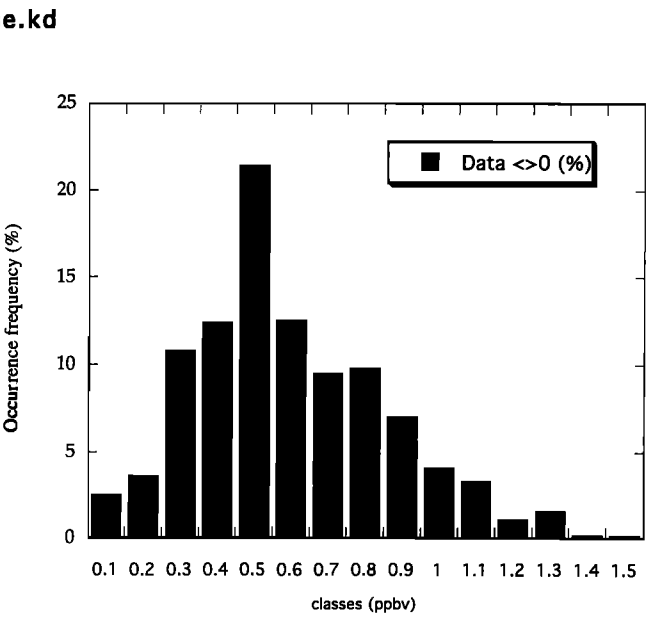


**Figure 2.** Distributions of gas phase $H_2O_2$ mixing ratio in near-surface air determined aboard NOAA ship *Malcolm Baldrige* for 160–179 Julian days (June 8 to 27, 1992) during the ASTEX/MAGE.

find such strong correlation between $H_2O_2$ and $NO_x$ chemistry as it is observed in an urban environment.

For transport times longer than 2 days, we lose the signature of pollution, and we conclude that in these cases the variability of $H_2O_2$ should be mainly controlled by local factors. We deduce that $H_2O_2$ cannot be used as a tracer for clean air masses in the atmospheric marine boundary layer, as it could be over the continent near polluted regions.

### Diurnal Variations of $H_2O_2$ Mixing Ratio

After having discussed $H_2O_2$ data for the entire ASTEX/MAGE experiment, we now turn to the discussion of individual $H_2O_2$ diurnal cycles. Such cycles are only likely to be observed when all parameters controlling $H_2O_2$ are more or less stable (especially no rain events and no change of air mass origin). Diurnal variations can also be observed during some of the periods with a strong $H_2O_2$ trend, but they are much less pronounced and cannot be used for the analysis we present in the following.

As described previously, diurnal variations have been observed during periods (PER) 1, 2, and 3 (=PER A) of the MAGE experiment (Table 2). PER 2 comprises three successive daily cycles and has been split into three subperiods (2.1, 2.2, 2.3), each corresponding to a single cycle.

All data have been averaged on an hourly basis. The set of these five different diurnal variations is reported in Figure 3a. We have also reported in Figure 3b the diurnal variation of $H_2O_2$ calculated over the whole period of the ASTEX/MAGE experiment, the average variation for PER A, the diurnal variation observed by *Ayers et al.* [1992] at Cape Grim monitoring site (Tasmania, 41°S) during January 1992 (monthly average), and the one observed by *Thompson et al.* [1993] during the Soviet-American Gas and Aerosol (SAGA) III experiment. This last experiment has been performed during the winter of 1990 in the equatorial region of the Pacific Ocean. To compare all these sequences, we have plotted in Figure 4 the daily $H_2O_2$ variation normalized to the mean value of $H_2O_2$ for each day (Figure 4a) and for each long duration period, namely, MAGE, PER A, SAGA III, and Cape Grim (Figure 4b).

All curves of Figure 4 show a very similar pattern with a minimum around 0700 and 1000 and a maximum between 1700 and 2000. The relative amplitude (Figures 4a and 4b) of the daily variations are very similar and range between 20 and 40% around the mean values of $H_2O_2$. Because of averaging, daily cycles presented in Figure 4b are less pronounced than the individually observed in Figure 4a. We note that for all three experiments (Cape Grim, SAGA III, and the averaged PER A/MAGE), average daily cycles are very similar to each other (Figures 3b and 4b).

**Table 1.** Statistical Parameters of $H_2O_2$ (in ppbv)

| Period | Arithmetic Mean | Standard Deviation | Geometric Mean | Median | Distribution |
|---|---|---|---|---|---|
| June 8–27 | 0.63 | 0.28 | 0.55 | 0.60 | lognormal |
| Lag 1 | 0.80 | 0.21 | 0.77 | 0.80 | lognormal |
| Lag 2 (global) | 0.59 | 0.29 | 0.52 | 0.54 | bimodal |
| Lag 2 | 0.39 | 0.12 | 0.37 | 0.37 | mode 1 |
| Lag 2 | 0.95 | 0.11 | 0.94 | 0.95 | mode 2 |

**Table 2.** Definition of Meteorological Periods and Typical $H_2O_2$ Periods

| Notation | Approximate Times | Description | Types |
|---|---|---|---|
| | *Periods Defined by Air Mass Trajectories* | | |
| U1 | 160.0–163.2 | uninhabited North America | U |
| U2 | 163.8–165.4 | W winds central North America | U |
| C3 | 165.4–166.0 | clean marine | C |
| M2 | 166.0–167.12 | mixed marine/North America | M |
| C4 | 167.12–167.5 | clean marine | C |
| M3 | 167.5–167.75 | mixed marine/North America | M |
| C5 | 167.75–168.75 | clean marine | C |
| I3 | 168.8–171.7 | West Europe/Africa | I |
| M4 | 171.7–172.3 | mixed marine/northern Europe | M |
| I4 | 172.3–174.5 | northern Europe | I |
| M5 | 174.5–177.8 | mixed marine/North America | M |
| C6 | 177.8–178.6 | clean marine | C |
| M6 | 178.6–181.0 | mixed marine/North America | M |
| | *Periods Defined by $H_2O_2$ Pattern* | | |
| PER 1 | 161.2–162.2 | diurnal variation | A |
| PER 2 | 172.7–175.7 | diurnal variation | A |
| PER 3 | 176.2–177.2 | diurnal variation | A |

$H_2O_2$ also shows an average diurnal variation for the whole MAGE experiment and this despite the crude averaging. This daily variation of $H_2O_2$ during MAGE could be considered as a climatological variation for June 1992. However, its minimum and its maximum are slightly shifted forward in time when compared with the averaged PER A or with those of Cape Grim and SAGA III. They occur at 1000 and 2100, respectively, for the MAGE period.

During nighttime, $H_2O_2$ has no known important chemical loss mechanism. The fact that a strong $H_2O_2$ decrease is, however, observed during the night thus can only be due to heterogeneous and physical removals (dry deposition, absorption on sea-salt particles or cloud droplets, precipitation scavenging). Without these loss processes, $H_2O_2$ mixing ratio would probably be much higher than observed in the marine boundary layer and its diurnal cycle less pronounced. This can, in fact, be observed in the free troposphere [*Heikes*, 1992]. On the basis of the diurnal cycles shown in Figures 4a and 4b, we will now try to quantify a first-order rate coefficient ($\tilde{K}_h$) for heterogeneous $H_2O_2$ loss in the marine boundary layer.

It is assumed that $\tilde{K}_h$ is constant during the night, that advection can be neglected, and that no significant entrainment through the top of the marine boundary layer (MBL) occurs. The validity of these assumptions will be discussed later. Thus the equation describing the temporal evolution of $H_2O_2$ mixing ratio during nighttime can be written as follows:

$$d[H_2O_2]/dt = -\tilde{K}_h[H_2O_2] \quad (2)$$

Using average nighttime $H_2O_2$ mixing ratio $\langle[H_2O_2]\rangle_{night}$ and tendency $\langle d[H_2O_2]/dt\rangle_{night}$, a loss timescale $\tau_{loss}$ is inferred:

$$\tau_{loss} = \tilde{K}_h^{-1} = -\langle[H_2O_2]\rangle_{night}/\langle d[H_2O_2]/dt\rangle_{night} \quad (3)$$

The estimation of $\tau_{loss}$ is done for measurements taken between 1800 and 0600, which is the same time interval as has been used by *Ayers et al.* [1992] to derive a $\tilde{K}_h$ for the Cape Grim data set. The slope of the decrease, the mean value, the standard deviation during nighttime and the inferred $\tilde{K}_h$ are given in Table 3 for each considered period. We observe that the day-to-day variability displays values between $0.5 \times 10^{-5}$ $s^{-1}$ and $1.6 \times 10^{-5}$ $s^{-1}$. The mean value for all the PER A daily cycles is $0.997 \times 10^{-5}$ $s^{-1}$ which is very close to the $1.0 \times 10^{-5}$ $s^{-1}$ value deduced by *Ayers et al.* [1992] for January 1992 at Cape Grim, where seasonal and marine conditions may be very similar to those encountered during ASTEX/MAGE. For SAGA III we found $\tilde{K}_h = 0.7 \times 10^{-5}$ $s^{-1}$. For the entire period of the ASTEX/MAGE experiment its mean value is $0.92 \times 10^{-5}$ $s^{-1}$. Of course, calculations for shorter portions of the diurnal cycle during nighttime yield slightly different results. It appears that the loss rate derived from mean values for the three experiments range only between 0.7 and $1.0 \times 10^{-5}$ $s^{-1}$. The low variability of this parameter is quite surprising if we consider the different areas and seasons it has been calculated for.

### Discussion of Different $H_2O_2$ Physicochemical Processes

So far, we stated the existence of a nonchemical $H_2O_2$ loss, but we did not investigate its origin. Now we are going to discuss in detail all the processes which can influence the $H_2O_2$ variability. The time evolution of $H_2O_2$ is given by the following general equation:

$$\frac{d[H_2O_2]}{dt} = \underbrace{(P1 - L1 * [H_2O_2])}_{\text{Photochemistry}} + \underbrace{P2 - L2 * [H_2O_2]}_{\text{Transport, Physics}} \quad (4)$$

where $P_1 = k_1 [HO_2^{\cdot}]^2$, and $L_1 = (k_{16} [OH] + J_{17})$ describe photochemical processes, with $k_1$ being the second-order rate

**Table 3.** Average Nighttime $H_2O_2$ Mixing Ratio (ppbv), Decreasing Slope, and $\tilde{K}_h$ for Different Episodes of the PER A type, after Averaging Over all PER A Episodes, for the MAGE Experiment Period (⟨160–180⟩, for Cape Grim [after *Ayer et al.*, 1992], and for SAGA II Experiment [after *Thompson et al.*, 1993]

| | PER 1 | PER 2.1 | PER 2.2 | PER 2.3 | PER 3 |
|---|---|---|---|---|---|
| Average nighttime $H_2O_2$ mixing ratio (ppbv) | 1.04 | 0.64 | 0.62 | 0.57 | 0.91 |
| Slope, ppb $h^{-1}$ | −3.48E−02 | −3.79E−02 | −1.04E−02 | −2.81E−02 | −2.46E−02 |
| $\tilde{K}_h$, $s^{-1}$ | 9.26E−06 | 1.64E−05 | 4.70E−06 | 1.36E−05 | 7.53E−06 |
| | ⟨PER A⟩ | ⟨160–181⟩ | Cape Grim | SAGA III | |
| Average nighttime $H_2O_2$ mixing ratio, ppbv | 0.76 | 0.68 | 0.88 | 0.62 | |
| Slope (ppb $h^{-1}$) | −2.72E−02 | −2.25E−02 | −2.19E−02 | −1.49E−02 | |
| $\tilde{K}_h$, ($s^{-1}$) | 9.97E−06 | 9.18E−06 | 6.93E−06 | 6.70E−06 | |

Read −3.48E−02 as $-3.48 \times 10^{-2}$. Calculations are done for 1800–0600 time period

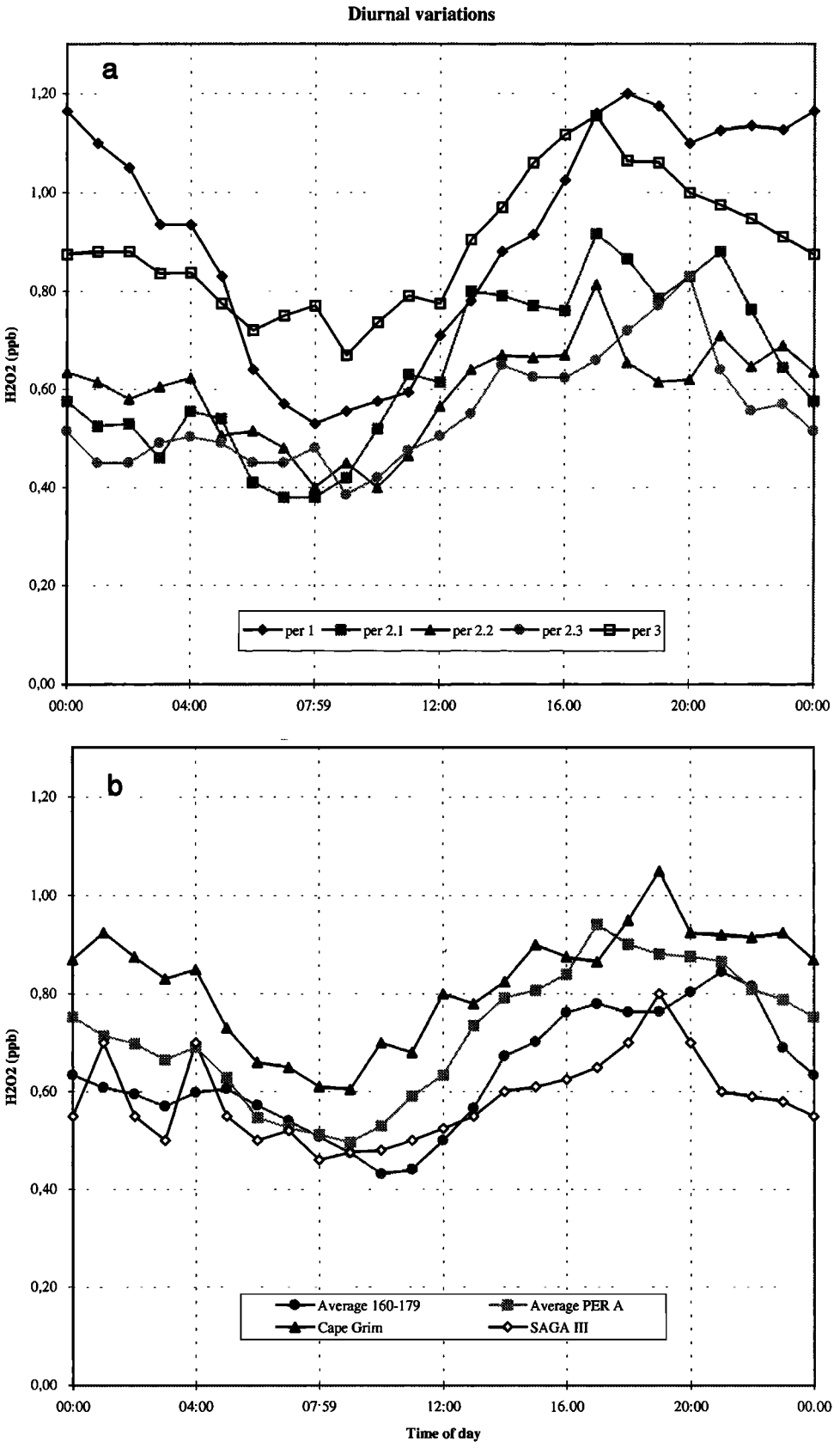


**Figure 3.** (a) Diurnal variations of $H_2O_2$ mixing ratio during the different PER A episodes. (b) Averaged diurnal variation at Cape Grim [*Ayers et al.*, 1992], averaged diurnal variation during PER A episodes, and during the MAGE experiment.

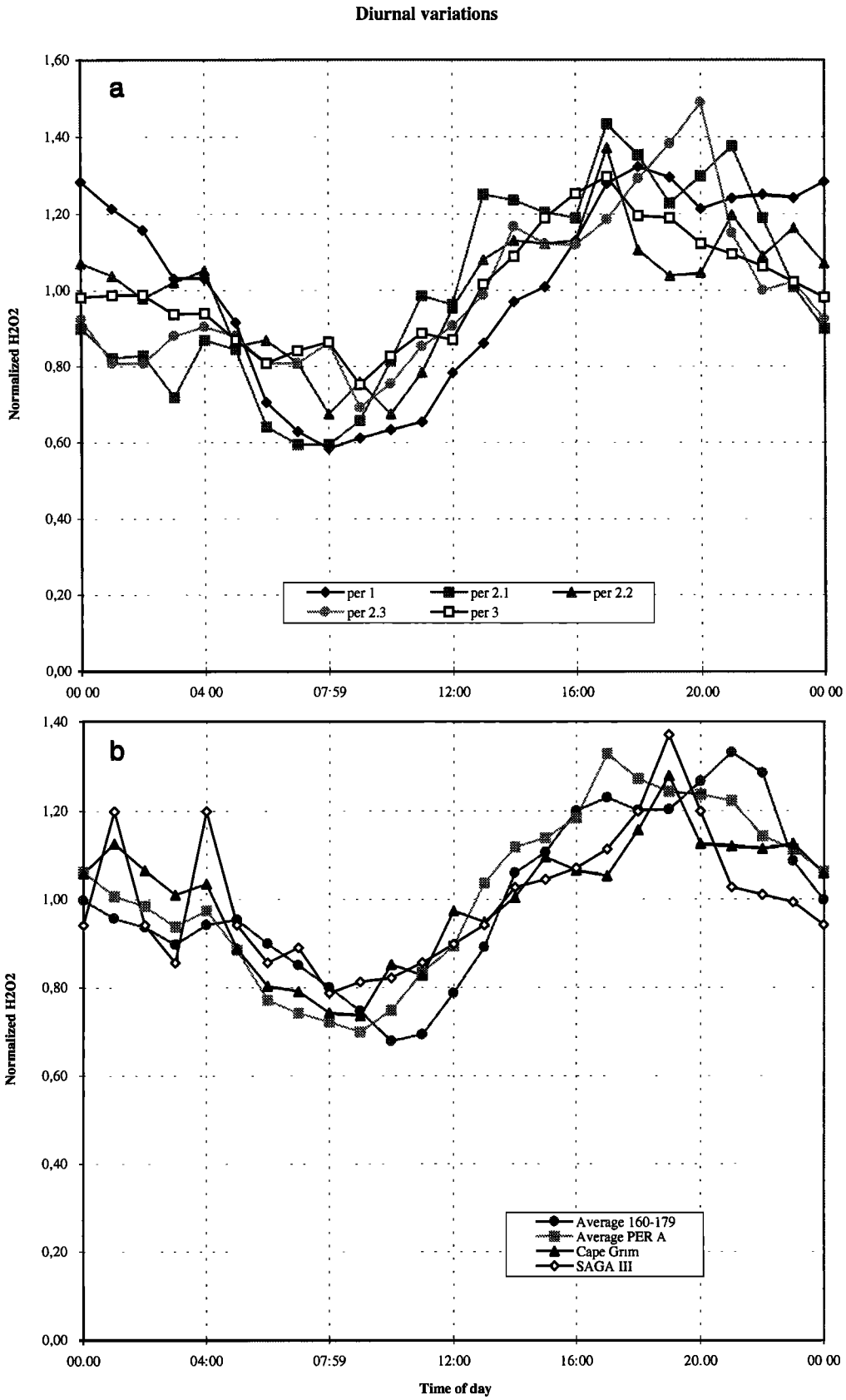


**Figure 4.** Same as Figure 3 with normalized $H_2O_2$ mixing ratio.

coefficient for recombination of $HO_2^{\cdot}$ radicals, $k_{16}$ the rate of (R16), $J_{17}$ the photolysis frequency of (R17).

$P_2 = -(\vec{V}_H - \vec{V}_{ship}) * \vec{\nabla}[H_2O_2] + (\omega_e/z_i) * [H_2O_2]^{ft}$, and $L_2 = (v_{dep} + w_e)/z_i + K_h$. These terms describe physical processes. The first term of $P_2$ represents the horizontal advection, and its second term is due to entrainment processes at the top of the boundary layer [*Lenschow et al.*, 1981, 1982]. $\vec{V}_H$ is the horizontal wind vector, $\vec{V}_{ship}$, the horizontal speed vector of the MB ship, $w_e$, the entrainment velocity, and $[H_2O_2]^{ft}$ the concentration of $H_2O_2$ in the free troposphere, $K_h$ is the first-order rate coefficient for heterogeneous and physical removals (absorption on particles such as sea-salt particles, aerosols, cloud droplets). Note that $\tilde{K}_h = v_{dep}/z_i + K_h$. The marine boundary layer is assumed to be well mixed, so that (4) is describing the temporal evolution of $H_2O_2$ in the whole boundary layer column up to the inversion height $z_i$.

It has been tried to derive estimates for the production and loss terms $P1$, $P2$, $L1$, and $L2$ by applying a quasi-Newton optimization method [*Numerical Algorithm Group (NAG)*, 1990] to fit (4) with experimental data for each selected period (PER A), assuming that $P1$ and $L1$ are proportional to the diurnal variation of UV radiation and that $L2$ and $P2$ are constant during the selected period. Unfortunately, this method has not been very successful, probably due to the high variability in the data. However, for data taken in a Lagrangian context, such an approach would be more promising, allowing then for a more detailed analysis of the different processes controlling $H_2O_2$ mixing ratios.

As it is not possible to gain further insight into the different $H_2O_2$ physicochemical processes using the present data, we will attempt to discuss the different terms in the light of generally known facts.

### Evaluation of $P_i$ and $L_i$ Terms

Photochemical production

$$P_1 = k_1[HO_2^{\cdot}]^2$$

According to *Atkinson et al.* [1992], $k_1$ can be expressed as follows: $k_1 = ((K_1(T) + K_2(P, T)) \times f_w(T, [H_2O])$, where $K_1(T)$ represents the bimolecular term, $K_2(P, T)$ is a pressure dependent term, and $f_w(T, [H_2O])$ is a water dependent factor. $T$ is air temperature (Kelvin), and $[H_2O]$ is the water vapor concentration (molecules $cm^{-3}$). Using $T$ and $P$ observed during the ASTEX/MAGE experiment, $k_1$ can be written as follows: $k_1$ ($cm^3$ $molecule^{-1}$ $s^{-1}$) = $(2.79 \pm 0.03) \times 10^{-12} \times (1 + 1.4 \times 10^{-21}$ $[H_2O] \times \exp(2200/T))$. During the experiment, temperature and relative humidity ranged between 16–22°C and 50–95%, respectively, leading to a minimum of $4.8 \times 10^{-12}$ and to a maximum of $6.7 \times 10^{-12}$ $cm^3$ $molecule^{-1}$ $s^{-1}$ for $k_1$, its mean value being $5.8 \pm 0.3 \times 10^{-12}$ $cm^3$ $molecule^{-1}$ $s^{-1}$. The daily mean $[HO_2^{\cdot}]$ mixing ratio is expected to range around 10 ppt ($2.7 \times 10^8$ molecules, $cm^{-3}$) (M. Kanakidou, personal communication), and the estimation of $P_1$ is thus $4.2 \times 10^5$ molecules $cm^{-3}$ $s^{-1}$ ($1.6\ 10^{-5}$ ppb $s^{-1}$).

Transport

$$P_2 = -(\vec{V}_H - \vec{V}_{ship}) * \vec{\nabla}[H_2O_2] + \frac{\omega_e}{Z_i} * [H_2O_2]^{ft}$$

The mean wind speed rarely exceeded 10 m $s^{-1}$, the ship speed is estimated to about 7 m $s^{-1}$, and the average latitudinal gradient is about 45 ppt/° [*Jacob and Klockow*, 1992]. Thus the maximum horizontal advection term can be estimated to around $1.8 \times 10^5$ molecules $cm^{-3}$ $s^{-1}$ ($7 \times 10^{-6}$ ppb $s^{-1}$). We see that the horizontal advection term could account for as much as half of the photochemical production and that except during the Lagrangian experiment should be taken into account.

The second term of $P_2$ represents the inputs from the free troposphere. Its estimation is quite difficult because our knowledge of $w_e$, $z_i$, and $H_2O_2$ in the free troposphere ($[H_2O_2]^{ft}$) is very poor during the ASTEX experiment. What we know is the following:

1. The mixing height $z_i$ was only available during the Lagrangian experiments and ranged between 500 and 1600 m during lag 1 and between 1800 and 2200 m during lag 2.

2. Using three different methods, *Bretherton et al.* [1995] estimated $w_e$ during Lagrangian experiments. They came to a consensus of $0.7 \pm 0.3$ cm $s^{-1}$ and $0.6 \pm 0.3$ cm $s^{-1}$ for $\omega_e$ during lags 1 and 2, respectively. On the basis of these estimates we get

$$2.5 \times 10^{-6} \le \omega_e/z_i \le 2.0 \times 10^{-5}\ s^{-1} \text{ during lag 1}$$

$$1.4 \times 10^{-6} \le \omega_e/z_i \le 5 \times 10^{-6}\ s^{-1} \text{ during lag 2}$$

3. It is also difficult to estimate at least the order of magnitude of $[H_2O_2]^{ft}$ because no $H_2O_2$ measurements in altitude were performed during ASTEX/MAGE. Several studies have reported a high variability (0.02 to 6 ppb) of $H_2O_2$ in altitude (see Table 4). Its concentration is usually larger in the free troposphere than in the MBL. The MOGUNTIA model calculates a zonal mean of 1.1 ppb at 2 km for June. During the MAGE experiment our maximum value observed in the MBL was 1.5 ppb and could be interpreted as an input from the free troposphere. Thus we retain this value of 1.5 ppb for $[H_2O_2]^{ft}$. This leads to an estimate of the second term of $P_2$ to

$$4.4 \times 10^4 \le \omega_e/z_i * [H_2O_2]^{ft} \le 6.5\ 10^5 \text{ molecules cm}^{-3}\ s^{-1}$$

or

$$(2.1 \times 10^{-6} \le \omega_e/z_i * [H_2O_2]^{ft} \le 3.0 \times 10^{-5} \text{ ppb } s^{-1})$$

We see that this term could be as large as or even greater than the photochemical production.

Photochemical loss

$$L1 * [H_2O_2] = (k_{16}[OH] + J_{17}) * [H_2O_2]$$

Using average values for OH and $H_2O_2$, respectively, equal to $1.0 \times 10^6$ molecules $cm^{-3}$ [*Thompson*, 1995] and 0.6 ppb (this work), $k_{16} = 1.7 \pm 0.1\ 10^{-12}$ molecules $cm^{-3}$ $s^{-1}$ [*Atkinson et al.*, 1992]; the mean daytime value of $J_{17} = 7 \times 10^{-6}$ $s^{-1}$; we obtain for $L1 * [H_2O_2]$ an estimation of $1.0 \times 10^5$ molecules $cm^{-3}$ $s^{-1}$ ($3.9 \times 10^{-6}$ $ppbs^{-1}$). Compared to the processes described above, this term could be neglected in a first approximation.

Physical loss processes

$$L_2 * [H_2O_2] = ((v_{dep} + \omega_e)/z_i + K_h) * [H_2O_2]$$

This is probably the most difficult term to be estimated because it involves heterogeneous processes like dry deposition or adsorption onto particles or export to the free troposphere. The term $\omega_e/z_i$ has been discussed previously. In fact, the weight of the entrainment process is strongly linked to the gradient of $H_2O_2$ at the interface. During MAGE we have seen

**Table 4.** Previous $H_2O_2$ Concentrations

| Measurement | Sampling Period | Sampling Site | Sampling Height, m | Analytical Technique | Detection Limit, ppbv | $H_2O_2$ Variability, ppbv | References |
|---|---|---|---|---|---|---|---|
| Airborne | June 1987 | 40°–44°N, 74°–82°W | sol → 4000 | FL[a] | 0.05 | 0.6–3.6 | *Van Valin et al.* [1990] |
| (by aircrafts) | June 1987 | 40°W, 82°W | 500 → 5500 | FL | 0.2 | <0.2–7 | *Daum et al.* [1990] |
| | Jan.–March 1986 | 34°N, 80°N | 200 → 4200 | FL | 0.2 | 0.2–2.4 | *Barth et al.* [1989] |
| | Aug.–Sept. 1988 | 37°–42°N, 76°–84°W | 100 → 3500 | FL | 0.2 | 0.2–5.9 | *Tremmel et al.* [1993] |
| | July–Aug. 1988, March–April 1990 | 52°N, 85°W | 600, 1200, 1400, 2500, 3000 | FL | 0.1 | 0.1–6 | *MacDonald et al.* [1991] |
| | Jan. 1991 | 60° S–60°N | 0 → 11000 | FL | 0.2 | 0.42–6.31 | *Perros* [1993] |
| | 1988 | 38.5°N, 92°W | 720 → 3700 | FL | ··· | 0.07–6.6 | *Ray et al.* [1992] |
| Airborne (by balloon and glider) | July 1990 and 1991 | 46° N, 8° E | 0 → 2200 → 4100 | FL | ··· | 0.2–5.6 | *Sigg et al.* [1991] |
| Ground level | July 1989 | 63° 26′N, 13° 06′E | 1250 | FL | 0.2 | 0.05–0.16 | *Noone et al.* [1991] |
| | Aug. 1985 to Sept. 1988 | 34°N, 118°W | 1.5, 10, 15, 1378, 1790 | FL | ··· | 0.03–1.35, 0.20–2.04 0.43–1.72, 0.12–0.78 | *Sakugawa and Kaplan* [1989] |
| | April 1987 | 52°N, 1°W | 2 | CL, (lum)[b] | 0.06 | 0.06–3.5 | *Dollard et al.* [1989] |
| | May 1988 to July 1991 | 48°N, 12°E | 2 → 50 | CL, (TCPO)[c] | 0.85 | 0.036–1.3 | *Kins* [1991] |
| | July 1990 and 1991 | 46° 32′N, 7° 59′E | 600, 3454 | FL | 0.003–0.01 | 1–6 | *Lehmann et al.* [1991] |
| | Jan.–March 1988 | 42°N, 13°E | sol | denuder tub | 0.07 | 0.04–0.43 | *Possanzini et al.* [1988] |
| | July 1987 to 1990 | 52°N, 1°W | 2 | CL, (lum) | 0.14 | 0.14–0.97 | *Dollard and Davies* [1992] |
| | summer–winter 1986 | 36° 39′N, 81° 38′W | 1689 | FL | 0.02 | 0.02–2.6 | *Olszyna et al.* [1988] |
| | March–Sept. 1986 and 1987 | 44°–36°N, 73°–81°W | 1483 et 1689 | FL | 0.2 | 0.5–6.1 | *Meagher et al.* [1990] |
| | May–Sept. 1988 | 36°N, 79°W | 1776, 2022 | FL | 0.1 | 0.1–4.18 | *Claiborn and Aneja* [1991] |
| | Feb. 1991 to March 1992 | 41°S, 146°E | 100 | FL | 0.02 | 0.2–1.4 | *Ayers et al.* [1992] |
| | May 1988 | 19° 32′N, 155° 36′W | 3400 | FL | 0.03 | 0.03–3.23 | *Heikes* [1992] |
| | March–April 1988 | 13°S, 38°W | 1–1.5 | CL, (TCPO) | 0.25 | 0.2–3.9 | *Jacob et al.* [1990] |
| | summer 1985/1986 | 51° 30′N, 7° 30′E | 1–1.5 | CL, (TCPO) | 0.25 | 0.01–0.6 | *Jacob et al.* [1990] |
| | Sept.–Oct. 1988 | 54°N–32°S | 3 | CL, (TCPO) | 0.25 | 0.22–3.5 | *Jacob and Klockow* [1992] |
| | Feb.–March 1990 | 20°N–10°S | 10 | FL | | 0.4–0.8 | *Thompson et al.* [1993] |
| MAGE | June 1992 | 32.5°N, 22°W | 15 | FL | 0.05 | 0.05–1.5 | this work |

[a]Fluorescence.
[b]Luminol chemiluminescence.
[c]Chemiluminescence of bis (2,4,5, trichloro-6-phenyl oxalate).

that it could be of the order of 1 ppb leading to a significant role in replenishing the MBL. On the other hand, *Heikes* [1992] has observed that the mixing ratio in the MBL at Mauna Loa Observatory during the Mauna Loa Observatory Photochemistry Experiment follows the mixing ratio of the free troposphere. Their difference between the marine boundary layer and the free troposphere is about 0.5 ppbv which leads to a contribution 2 times smaller than estimated above.

On the basis of the diurnal variations we have been able to give an estimate of the term $\bar{K}_h = K_h + v_{dep}/z_i$. We have seen that this process could be of the same order of magnitude or even larger than the chemical production or/and than the exchanges between the MBL and the free troposphere.

Thus by the analysis of all those processes, it is clearly difficult to attribute the derived $\bar{K}_h$ to one precise process, and we point out the need of a full mesoscale meteorological and chemical model for a complete understanding of the variability of $H_2O_2$ in the MBL. Furthermore, this analysis points out the need of a best estimate of $H_2O_2$ in the free troposphere and of $\omega_e/z_i$. This requires a study which will involve simultaneously both surface and vertical measurements.

For the time being, as seen from the relatively low variability of $\bar{K}_h$ obtained for the different measurement campaigns, an approximate value of $0.7 \times 10^{-5}$ to $1.0 \times 10^{-5}$ ($s^{-1}$) may be used for modeling purposes, in order to close the $H_2O_2$ budget in the marine boundary layer.

## Conclusion

Hydrogen peroxide ($H_2O_2$) mixing ratios in near-surface air were measured continuously onboard the research vessel *Malcom Baldrige* during the ASTEX/MAGE experiment in the eastern subtropical North Atlantic from June 8 to 27, 1992 (Julian days 160 to 179). Mixing ratios ranged between 0.05 and 1.5 ppbv with a high variability. The mean value and standard deviation of the data for the whole period were $0.63 \pm 0.28$ ppbv. These values are in good agreement with previous observations made in the same region by *Jacob and Klockow* [1992] and *Weller et al.* [1993]. Although a high value of $H_2O_2$ (1.5 ppbv) was observed during lag 1 at Julian day 165.95 (UTC), it appears that the $H_2O_2$ mixing ratios generally observed during June 1992 are representative of the eastern subtropical North Atlantic Ocean atmosphere in late spring.

No systematic correlations were observed between $H_2O_2$ and meteorological parameters, while for some tracers ($^{222}Rn$, black carbon, and CO), significant correlations were observed only when air masses came from Europe and had a travel time less than 2 days.

$H_2O_2$ times series is analyzed according to sequences having a characterized diurnal cycle. It is pointed out that all these diurnal variation periods show the same shape with a minimum between 0700 and 0900 and a maximum between 1700 and 1900. The relative variation of the $H_2O_2$ mixing ratio ranges between 20 and 40% around the mean value.

A diurnal variation of $H_2O_2$ mixing ratio was also observed during the overall period of MAGE with a maximum between 1630 and 2100 and a minimum around 1030 LT. From all of these results, a first-order reaction coefficient for physical removal of about $1.\times 10^{-5}\ s^{-1}$ is estimated. This mean value is found to be identical to the value of *Ayers et al.* [1992] calculated at Cape Grim in the southern hemisphere and relatively close to that derived for the SAGA III experiment in the equatorial Pacific Ocean. The day-to-day variability is found to be ±50% around the mean value. This coefficient is discussed according to different physical and chemical processes, including the entrainment velocity observed during both Lagrangian experiments.

In this study, we have shown that $H_2O_2$ cannot be considered as an air mass tracer in the marine atmospheric boundary layer. We have pointed out the crucial role of the heterogeneous processes. These processes should be more investigated in the future. We have pointed out the need of $H_2O_2$ measurements in altitude to investigate the exchanges between the free troposphere and the MBL. Finally, a complete meteorological-chemical model will be necessary to describe in detail the variability of $H_2O_2$ in the marine atmospheric boundary layer.

**Acknowledgments.** We express our sincere thanks to Barry Huebert for his effort in coordinating the MAGE project. We are in dept to anonymous reviewers for their useful comments and suggestions. We also thank Pierre Weiss, Gale Variot, Robert Calvert, Charlie Fischer, and Antonio Mendez for technical assistance and Captain C. Y. Molyneaux and the *Malcolm Baldrige* crew for their support aboard ship. This research was supported by the CNRS/Programme Environnement (PACB) and the NOAA Climate and Global Change Program and is a contribution to the International Global Atmospheric Chemistry (IGAC) core project of the International Geosphere-Biosphere Programme (IGBP). This is CFR contribution 1706.

## References

Atkinson, R., D. L. Baulch, R. A. Cox, R. F. Hampson, J. A. Kerr, and J. Troe, Evaluated kinetic and photochemical data for atmospheric chemistry, Supplement IV, *J. Phys. Chem. Ref. Data*, *21*(6), 1125–1568, 1992.

Ayers, G. P., S. A. Penkett, R. W. Gillett, A. B. Bandy, I. E. Galbally, C. P. Meyer, C. M. Ellsworth, S. T. Bentley, and B. W. Forgan, Evidence for photochemical control of ozone concentrations in unpolluted marine air, *Nature*, *360*, 446–449, 1992.

Barth, M. C., D. A. Hegg, P. V. Hobbs, J. G. Walega, G. L. Kok, B. G. Heikes, and A. L. Lazrus, Measurements of atmospheric gas-phase and aqueous phase hydrogen peroxide concentrations in winter on the East Coast of the United States, *Tellus*, *41B*, 62–69, 1989.

Bateman, H., Solution of a system of differential equations in the theory of radioactive transformations, *Proc. Cambridge Phil. Soc.*, *15*, 423, 1910.

Becker, K. H., K. J. Brockmann, and J. Bechara, Production of hydrogen peroxide in forest air by reaction of ozone with terpenes, *Nature*, *346*, 256–258, 1990.

Bretherton, C. S., and R. Pincus, Cloudiness and marine boundary layer dynamics in the ASTEX Lagrangian experiments, I, Synoptic setting and vertical structure, *J. Atmos. Sci.*, *52*(16), 2707–2723, 1995.

Bretherton, C. S., P. Austin, and S. T. Siems, Cloudiness and marine boundary layer dynamics in the ASTEX Lagrangian experiments, II, Cloudiness, drizzle, surface fluxes, and entrainment, *J. Atmos. Sci.*, *52*(16), 2724–2735, 1995.

Cachier, H., M. Bremond, and P. Buat-Ménard, Organic and black carbon aerosols over marine regions of the Northern Hemisphere, in *Proceedings of the International Conference on Atmospheric Chemistry*, edited by L. Newman and C. S. Kiang, pp. 249–261, Brookhaven Natl. Lab., Upton, N. Y., 1990.

Calvert, J. G., and W. R. Stockwell, Acid generation in the troposphere by gas-phase chemistry, *Environ. Sci. Technol.*, *17*, 428A–443A, 1983.

Calvert, J. G., A. Lazrus, G. L. Kok, B. G. Heikes, J. G. Walega, J. Lind, and C. A. Cantrell, Chemical mechanisms of acid generation in the troposphere, *Nature*, *317*, 27–35, 1985.

Carsey, T. P., M. L. Farmer, C. J. Fischer, A. Mendez, A. A. Pszenny, V. B. Ross, P.-Y. Whung, M. Springer-Young, and M. P. Zetwo, Atmospheric chemistry measurements from the 1992 ASTEX/MAGE cruise, 30 May 1992 through 21 July 1992, Cruise number 91-126, *NOAA Data Rep., ERL AOML-26*, Natl. Oceanic and Atmos. Admin., Washington, D. C., 1994.

Claiborn, C. S., and V. P. Aneja, Measurements of atmospheric hy-

drogen peroxide in the gas phase and in cloud water at Mt. Mitchell, North Carolina, *J. Geophys. Res.*, *96*, 18,771–18,787, 1991.

Cox, R. A., and J. P. Burrows, Kinetics and mechanism of the disproportionation of $HO_2^{\cdot}$ in the gas phase, *J. Phys. Chem.*, *83*, 2560–2568, 1979.

Daum, P. H., T. J. Kelly, S. E. Schwartz, and L. Newman, Measurement of the chemical composition of stratiform clouds, *Atmos. Environ.*, *18*, 2671–2684, 1984.

Daum, P. H., L. I. Kleinman, A. J. Hills, A. L. Lazrus, A. C. D. Leslie, K. Busness, and J. Boatman, Measurement and interpretation of concentrations of $H_2O_2$ and related species in the upper midwest during summer, *J. Geophys. Res.*, *95*, 9857–9871, 1990.

Dodge, M. C., A comparison of three photochemical oxidant mechanisms, *J. Geophys. Res.*, *94*, 5121–5136, 1989.

Dollard, G. J., and T. J. Davies, Observations of $H_2O_2$ and PAN in a rural atmosphere, *Environ. Pollut.*, *75*, 45–52, 1992.

Dollard, G. J., F. J. Sandalls, and R. G. Derwent, Measurements of gaseous hydrogen peroxide in southern England during a photochemical episode, *Environ. Pollut.*, *58*, 115–124, 1989.

Ehhalt, D. H., and J. W. Drummond, The tropospheric cycle of $NO_x$, in *Chemistry of the Unpolluted and Polluted Troposphere*, edited by H.-W. Georgii and W. Jaeschke, pp. 219–251, Nato Adv. Stud. Inst., Corfu, Greece, 1981.

Finlayson-Pitts, B. J., and J. N. Pitts Jr., *Atmospheric Chemistry: Fundamentals and Experimental Techniques*, John Wiley, New York, 1986.

Gaffney, J. S., G. E. Streit, W. D. Spall, and J. H. Hall, Beyond acid rain, *Environ. Sci. Technol.*, *21*, 519–524, 1987.

Gunz, D. W., and M. R. Hoffmann, Atmospheric chemistry of peroxides: A review, *Atmos. Environ.*, *24A*, 1601–1633, 1990.

Hamilton, E. J., and R. R. Lii, The dependence on $H_2O$ and on $NH_3$ of the kinetics of the self-reaction of $HO_2^{\cdot}$ in the gas-phase: Formation of $HO_2$-$NH_3$ complexes, *Int. J. Chem. Kin.*, *9*, 875–885, 1977.

Hansen, A. D. A., R. S. Artz, A. A. P. Pszenny, and R. E. Larson, Aerosol black carbon and radon as tracers for air mass origin over the North Atlantic ocean, *Global Biogeochem. Cycles*, *4*(2), 189–199, 1990.

Heikes, B. G., Estimated uncertainty in hydrogen peroxide measurements using the catalase and peroxidase enzymes method, paper presented at the International Conference on the Generation of Oxidants on Regional and Global Scales, Univ. of East Anglia, Norwich, England, July 3–7, 1989.

Heikes, B. G., Formaldehyde and hydroperoxides at Mauna Loa Observatory, *J. Geophys. Res.*, *97*, 18,001–18,013, 1992.

Huebert, B. J., A. Pszenny, and B. Blomquist, The ASTEX/MAGE Experiment, *J. Geophys. Res.*, *101*, 4319–4329, 1996.

Jacob, D. J., and D. Klockow, Hydrogen peroxide measurements in the marine atmosphere, *J. Atmos. Chem.*, *15*, 353–360, 1992.

Jacob, D. J., T. M. Tavares, V. C. Rocha, and D. Klockow, Atmospheric $H_2O_2$ field measurements in a tropical environment: Bahia Brazil, *Atmos. Environ.*, *24A*, 337–382, 1990.

Kanakidou, M., and P. J. Crutzen, Scale problems in global tropospheric chemistry modelling: Comparison of results obtained with a three-dimensional model, adopting longitudinally uniform and varying emissions of NOx and NMHC, *Chemosphere*, *26*(1–4), 787–801, 1993.

Kins, L., Measurement of hydrogen peroxide in a forest area, in *Air Pollution Research Report 39, Field Measurements and Interpretation of Species Related to Photooxidants and Acid Deposition*, pp. 9–16, Neth. Organ. for Appl. Sci. Res., The Hague, 1991.

Kleinman, L. I., Photochemical production of peroxides in the boundary layer, *J. Geophys. Res.*, *91*, 10,889–10,904, 1986.

Kleinman, L. I., Seasonal dependence of boundary layer peroxide concentration: The low and high $NO_x$ regimes, *J. Geophys. Res.*, *96*, 20,721–20,733, 1991.

Koppmann, R., R. Bauer, F. J. Johnen, C. Plass, and J. Rudolph, The distribution of light nonmethane hydrocarbons over the mid-Atlantic: Results of the Polarstern Cruise ANT VII/1, *J. Atmos. Chem.*, *15*, 215–234, 1992.

Larson, R. E., and D. J. Bressan, Automatic radon counter for continual unattended operation, *Rev. Sci. Instrum.*, *49*, 965–969, 1978.

Lazrus, A. L., G. L. Kok, S. N. Gitlin, B. G. Heikes, and R. E. Shetter, Automated fluorometric method for hydrogen peroxide in air, *Anal. Chem.*, *58*, 594–597, 1986.

Lehmann, M., A. Sigg, B. E. Lehmann, and A. Neftel, $H_2O_2$ concentration during summer smog situations at the high alpine research station Jungfraujoch, in *Air Pollution Research Report 39, Field Measurements and Interpretation of Species Related to Photooxidants and Acid Deposition*, pp. 17–22, Neth. Organ. for Appl. Sci. Res., The Hague, 1991.

Lenschow, D. H., R. Pearson, and B. B. Stankov, Estimating the ozone budget in the boundary layer by use of aircraft measurements of ozone eddy flux and mean concentration, *J. Geophys. Res.*, *86*, 7291–7297, 1981.

Lenschow, D. H., R. Pearson, and B. B. Stankov, Measurements of ozone vertical flux to ocean and forest, *J. Geophys. Res.*, *87*, 8833–8837, 1982.

Liousse, C., Propriétés optiques du carbone suie, DEA Chimie de la Pollution Atmosphérique et Physique de l'Environnement, Univ. Paris 7, 1990.

Logan, J. A., M. J. Prather, S. C. Wofsy, and M. B. McElroy, Tropospheric chemistry: A global perspective, *J. Geophys. Res.*, *86*, 7210–7254, 1981.

MacDonald, A. M., K. G. Anlauf, H. A. Wiebe, W. R. Leaitch, C. M. Banic, M. F. Watt, K. J. Puckett, and B. Bregman, Measurements of aqueous and gaseous hydrogen peroxide in central Ontario, paper presented at Seventh Joint Conference on Applications of Air Pollution Meteorology, Air and Waste Manage. Assoc., New Orleans, La., January 14–18, 1991.

Masuch, G., A. Kettrup, R. K. A. M. Mallant, and J. Slanina, Effects of $H_2O_2$-containing acidic fog on young trees, *Int. J. Environ. Anal. Chem.*, *27*, 183–213, 1986.

Meagher, J. F., K. J. Olszyna, and F. P. Weatherford, The availability of $H_2O_2$ and $O_3$ for aqueous phase oxidation of $SO_2$, The question of linearity, *Atmos. Environ.*, *24A*, 1825–1829, 1990.

Numerical Algorithm Group (NAG) Limited, *Fortran Library Manual, Mark 14*, Oxford, England, 1990.

Noone, K. J., J. A. Ogren, K. B. Noone, and A. Hallberg, Measurements of hydrogen peroxide in a stratiform cloud, *Tellus*, *43B*, 280–290, 1991.

Olszyna, K. J., J. F. Meagher, and E. M. Bailey, Gas-phase, cloud and rain-water measurements of hydrogen peroxide at a high-elevation site, *Atmos. Environ.*, *22*, 1699–1706, 1988.

Penkett, S. A., B. M. R. Jones, K. A. Brice, and A. E. J. Eggleton, The importance of atmospheric ozone and hydrogen peroxide in oxidising sulphur dioxide in cloud and rain water, *Atmos. Environ.*, *13*, 123–137, 1979.

Perros, P. E., Large-scale distribution of hydrogen peroxide from aircraft measurements during the TROPOZ II experiment, *Atmos. Environ.*, *27A*, 1695–1708, 1993.

Piotrowicz, S. R., C. J. Fischer, and R. S. Artz, Ozone and carbon monoxide over the North Atlantic during a boreal summer, *Global Biogeochem. Cycles*, *4*(2), 215–224, 1990.

Possanzini, M., V. Di Palo, and A. Liberti, Annular denuder method for determination of $H_2O_2$ in the ambient atmosphere, *Sci. Total. Environ.*, *77*, 203–214, 1988.

Ray, J. D., C. C. Van Valin, and J. F. Boatman, The vertical distribution of atmospheric $H_2O_2$: A case study, *J. Geophys. Res.*, *97*, 2507–2517, 1992.

Sakugawa, H., and I. R. Kaplan, $H_2O_2$ and $O_3$ in the atmosphere of Los Angeles and its vicinity: Factors controlling their formation and their role as oxidants of $SO_2$, *J. Geophys. Res.*, *94*, 12,957–12,973, 1989.

Seiler, W., The Cycle of atmospheric CO, *Tellus*, *26*, 116–135, 1974.

Sigg, A., B. E. Lehmann, M. Lehmann, and A. Neftel, $H_2O_2$ measurements in the boundary layer over Switzerland during summer smog episodes, in *Air Pollution Research Report 39, Field Measurements and Interpretation of Species Related to Photooxidants and Acid Deposition*, pp. 23–27, Neth. Organ. for Appl. Sci. Res., The Hague, 1991.

Thompson, A. M., Measuring and Modeling the Tropospheric Hydroxyl Radical (OH), *J. Atmos. Sci.*, *52*(19), 3315–3327, 1995.

Thompson, A. M., et al., Ozone observations and a model of marine boundary layer photochemistry during SAGA 3, *J. Geophys. Res.*, *98*, 16,955–16,968, 1993.

Tremmel, H. G., W. Junkermann, and F. Slemr, On the distribution of hydrogen peroxide in the lower troposphere over the northeastern United States during late summer 1988, *J. Geophys. Res.*, *98*, 1083–1099, 1993.

Van Valin, C. C., M. Luria, J. D. Ray, and J. F. Boatman, Hydrogen peroxide and ozone over the northeastern United States in June 1987, *J. Geophys. Res.*, *95*, 5689–5695, 1990.

Walceck, C. J., A theoretical estimate of $O_3$ and $H_2O_2$ dry deposition over the Northeast United States, *Atmos. Environ.*, *21*, 2469–2659, 1987.

Weller, R., and O. Schrems, $H_2O_2$ in the marine troposphere and seawater of the Atlantic Ocean (48°N–63°S), *Geophys. Res. Lett.*, *20*, 125–128, 1993.

C. Abonnel, METEO-FRANCE, Centre National de la Recherche Météorologique, Centre d'Aviation Météorologique, 91228 Brétigny sur Orge Cedex, France.

B. Bonsang and M. Tsivou, Centre National de la Recherche Scientifique, Centre des Faibles Radio-activités, 91198 Gif sur Yvette, France.

T. Carsey and M. Springer-Young, NOAA, Atlantic Oceanographic and Meteorological Laboratory, 4301 Rickenbacker Causeway, Miami, FL 33149-1026.

D. Martin, Centre National de la Recherche Scientifique, Centre des Faibles Radio-activités, Orme des Merisiers-Batiment 709, 91198 Gif sur Yvette, France.

A. Pszenny, IGAC Core Project Office, Building 24-409, Massachusetts Institute of Technology, Cambridge, MA 02139-4307.

K. Suhre, Laboratoire d'Aérologie (UMR CNRS/UPS 5560), Observatoire Midi Pyrénées, 31400 Toulouse, France.

(Received October 10, 1994; revised August 12, 1996; accepted August 14, 1996.)